






Numerical Study on the Shear Capacity of PC Crane Beams in Uncertain Prestressing Tendons Anchorage Conditions

Rafał Walczak¹  and Wit Derkowski^{1,2}  

¹ Cracow University of Technology, Kraków, Poland
wit.derkowski@lnu.se

² Linnaeus University, Växjö, Sweden

Abstract. Numerical analyses relating to real-scale research of prestressed crane girders were carried out. Modelled beams had a low transverse reinforcement ratio. Moreover, the cable anchorages did not have any corrosion protection. Numerical analyses were conducted in phases, to simulate prestressed member operation (according to the research). Also, to simulate cables' anchorage failure, bonding transmission of the prestressing force and bonding anchorage of the tendons. A total of 29 numerical simulations were performed. Based on the calculation results, an analysis of the effect of the transverse reinforcement ratio and the effective prestressing force magnitude on the load carrying capacity of the girders was performed. Numerical analyses mapped experimental studies with satisfactory compliance. Therefore, analyses enabled research to be extended. Numerical analyses indicated, the reinforcement marginally affects the load carrying capacity of the investigated elements. Also, failure of the top cable's anchorage negligibly influences the load bearing capacity. On the other hand, the failure of bottom cables' anchorages significantly reduces the carrying capacity of the analysed elements.

Keywords: assessment · anchorages failure · numerical analysis · prestressed concrete · shear capacity

1 Introduction

Numerical calculations carried out in a proper way often provide much greater possibilities for the analysis of building structures than standard analytical models [1]. They can lead to a better prediction of the load-bearing capacity and deformability of the structure, while at the same time providing the possibility of obtaining more detailed information [2], such as the stress in the reinforcement, development of a crack pattern, correct recognition of the failure mode, etc. However, numerical modelling involves the possibility of erroneous analysis and therefore requires appropriate validation, preferably on the basis of experimental tests. Analysis of FEM models can be particularly useful in the assessment of existing concrete structures or their components, especially in situations of progressive change over time related to material ageing or corrosion progress [3].

Numerical analysis of post-tensioned, precast concrete beams in an emergency situation is presented in the paper. The analysis is complementary to the experimental tests on post-tensioned, precast crane girders dismantled after more than 50 years of exploitation presented at the *fib Congress, Oslo 2022* [4]. In these tests, the anchorage failure for one or two prestressing tendons was simulated. Due to the limited number of test specimens (only 9 beams in real scale were tested in the lab), numerical analysis enabled the research to be extended and, furthermore, to draw more generalised conclusions regarding the influence of the amount of transverse reinforcement on the shear capacity or the effects of anchorage failure of individual prestressing cables.

The developed numerical model, created in the DIANA FEA environment, makes it possible to obtain the information necessary to assess the safety of old post-tensioned concrete beams, even those in a close to failure situation. Such calculations can be used to make decisions about the possibility of continued use, thus becoming part of a more sustainable management of building infrastructure.

2 Description

2.1 Description of the Modelled Girders

The subject of the modelling were precast, post-tensioned concrete crane girders used in the bigger research program [4]. The elements were disassembled from the industrial hall after almost 60 years of use [5, 6]. The beams with an I-section of 800 mm in height and a modular span of 6.0 m were analysed. They were prestressed with five rectilinear 12Ø5 mm bonded tendons (four bottom tendons and a top one). The steel mechanical anchorages for the tendons at the ends of the beams had not been protected against corrosion. The longitudinal passive reinforcement consisted of 4Ø8 mm and 4Ø16 mm rebars respectively in the bottom and top flange – only smooth steel bars were used as a passive reinforcement. The beams were transversely reinforced with Ø8 mm stirrups at the irregular spacing between 160 mm – 400 mm. Therefore, the average transverse reinforcement ratio ranges from 0.19% to 0.28%. Consequently, the beams had a low transverse reinforcement ratio – in a few cases, the current standards' provisions for minimum transverse reinforcement are not met.

To investigate the influence of prestressing force magnitude and bonding anchorage on shear capacity, elements were diversified by the number of cables' anchorage failures (2 beams with failed two bottom anchorages, 4 beams with failed one top anchorage and 3 reference beams with all tendons proper anchored). The anchorage failure was simulated by cutting off utilising the circular saw. The anchorage failure simulation process as well as the bonding transmission research is reported in [7].

The beams were investigated in the three-point bending with a theoretical span of 5.80 m in three different load schemes to diversify the shear span-to-depth ratio (so-called shear slenderness a/d). The considered a/d ratio in the studies were 1.57, 2.61 and 3.66. In addition, the variation in the assessed quality of grout filling of the cable ducts was very high. Good, proper cement grout quality, as well as really bad quality and partial filling, was observed. As a result, the grout quality affected the bond anchorage of the tendons with fault anchors, thus, the prestressing force transmission magnitude.

2.2 Description of the FEA Model

Nonlinear FEM models were generated in DIANA FEA software. The analysis solution was iterated using the Newton-Raphson method, convergence was controlled by displacement and force equilibrium. Load steps were adjusted by the arc length control parameter. A 2D model was generated, with Q8MEM finite elements – plane stress state, isoparametric FE based on linear interpolation and Gaussian integration. The FE size was set to 30 mm in the final version of the model (Fig. 1). As a result, adequate solution accuracy with minimised solving time was achieved.

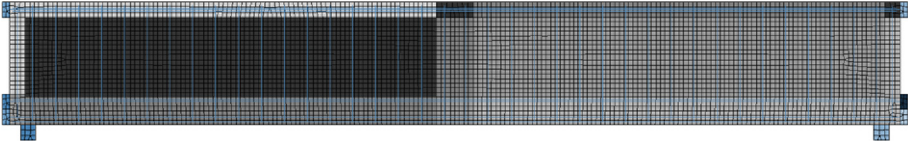


Fig. 1. Finite elements mesh of the numerical model.

FEM model calculations were carried out in the form of a phased analysis. For each phase of the element's operation, the specified boundary parameters were changed to reproduce the process of the respective tests. Moreover, to capture the actual behaviour of the tested elements in the numerical simulation. The computational process has been divided into 5 phases – see Table 1.

Table 1. Phased analysis of the numerical model.

Analysis phase	Modelled quality of cable duct grouting	
	Good (G)	Bad (B)
Phase I	Tensioning of the prestressing tendons (malleable bond-slip b-s parameters)	
Phase II	Anchoring of the tendons and injection of the cable ducts (assignment of the b-s parameters in relation to the grouting quality)	
Phase III'	Load application for the reference models with all functional anchorages of the prestressing cables	
Phase III	Removal of selected prestressing cables anchorages (bond transmission of pre-stressing force at transmission length) and initial loading of the element	
Phase IV	Initial b-s parameters degradation at the transformation to the cracked state of the beam section	Initial b-s parameters degradation at the transformation to the decompression state of the beam
Phase V	Subsequent b-s parameters degradation at loading of cracked section (118% of P_{cr} – cracking load)	Subsequent b-s parameters degradation at cracking load for a section with full prestressing force

III' is the final phase of the reference models analysis (all functional anchorages situation); Phase IV and V boundary limits were calibrated based on the experimental results (Fig. 3) as well as bond-slip parameters (compiled in Table 2).

Materials properties obtained on the basis of testing material samples (taken from tested girders [4]) were implemented directly into the model. Remaining parameters were assumed according to Model Code 2010 [8] and the literature [9–13]. Defined material models and properties were summarised in Table 2.

Table 2. Properties defined in the numerical models.

Modelled material	Property	Value	
Concrete – Total Strain Crack Model	Modulus of elasticity	34 900 MPa	
	Poisson's ratio	0.15	
	Mass density	2.40 T/m ³	
	Compressive strength	52.5 MPa	
	Tensile strength	2.0 MPa	
	Fracture energy	0.15 – 0.23 N/mm	
	Shear retention factor	0.5 – 0.8 (const.)	
Prestressing steel – multilinear relationship matched to the tested properties	Area of single prestressing tendon	236 mm ²	
	Modulus of elasticity	195 000 MPa	
	Poisson's ratio	0.30	
	Mass density	7.85 T/m ³	
	Ideal elasticity range limit	1200 MPa	
	Tensile strength	1760 MPa	
	Ultimate tensile strain	2.20%	
	Tendon prestressing force (stress)	150 kN (637 MPa)	
Tendon bond-slip perimeter G, (B)	100 mm (50 mm) *		
Reinforcement steel – multilinear relationship matched to the tested properties	Diameter of bottom longitudinal bars	8 mm	
	Diameter of top longitudinal bars	16 mm	
	Diameter of stirrups	8 mm	
	Modulus of elasticity	200 000 MPa	
	Poisson's ratio	0.30	
	Mass density	7.85 T/m ³	
	Yield stress	270 MPa	
	Tensile strength	360 MPa	
Ultimate tensile strain	20.60%		
Bond-slip parameters for tendons in phased analysis	Normal stiffness modulus	1000 N/mm ³	
	Shear stiffness modulus	5,9 N/mm ³	
Dörr interface failure model	Dörr b-s parameters	c [N/mm ²]	s [mm]
	I phase – G and B	$2 \cdot 10^{-5}$	5000
	II and III phase G, (B) *	5.0 (0.9)	10 (10)
	IV phase G, (B) *	2.5 (0.25)	10 (5)
	V phase G, (B) *	1.1 (0.14)	5 (0.1)

* parameters in brackets relate to (B) bad quality of duct grouting, otherwise – (G) good quality

Validation and calibration of the models were conducted based on the experimental results presented in [4]. Good consistency of numerical mapping of reference tests has

been achieved. Moreover, the model was able to accurately reflect all the phenomena observed in the experimental studies. A comparison of selected experimental results and numerical analyses is shown in the chapter 3 (Fig. 3).

After validation of the model, the following parametric analyses were carried out:

- influence of the transverse reinforcement ratio on shear capacity,
- influence of the effective prestressing force magnitude on shear capacity.

2.3 Performed Numerical Analyses

A total of 29 numerical simulations were carried out for different operating conditions of the girders (Fig. 2). The numerical research covered three different shear slendernesses (a/d), four patterns of cables' anchorage failure and two quality conditions for cable ducts' grout injection.

To identify the individual numerical analyses (N), a uniform nomenclature was applied: **N X-Y Z**, where: **X** is a type of static scheme referring to the shear slenderness ($1 - a/d = 1,57$; $2 - 2,61$; $3 - 3,66$); **Y** is a number of cables' anchorage failure; and **Z** refer to the grout quality, G – is a good quality, and B – bad quality. Also, models with varying stirrup reinforcement ratios were distinguished. The basic (designed) transverse reinforcement ratio of 0.42% ($\varnothing 8/150$ mm) was the reference. Models with twice reduced reinforcement ratio to the value of 0.21% (the average transverse reinforcement ratio in actual elements which is the minimum reinforcement ratio required by standards) are indicated by ' prime.

For example, **N 2–2 B'** identify a simulation of element tested in $a/d = 2,61$ static scheme with failure of two bottom tendons' anchorages (bad quality of the ducts' grouting) and reduced transverse reinforcement ratio to a minimal value. Table 3 contains the designations of the performed numerical analyses.

Table 3. Identification of the performed numerical analyses.

Analysed shear a/d ratio			Additional designations
$a/d = 1,57$	$a/d = 2,61$	$a/d = 3,66$	
N 1-0	N 2-0	N 3-0	
N 1-0'	N 2-0'	N 3-0'	G – good quality of the cable ducts' grouting
N 1-2 G	N 2-2 G	N 3-2 G	
N 1-2 B	N 2-2 B	N 3-2 B	B – bad quality of the cable ducts' grouting
N 1-2 G'	N 2-2 G'	N 3-2 G'	
N 1-2 B'	N 2-2 B'	N 3-2 B'	' – transverse reinforcement ratio reduced to 0.21% (corresponding to the minimal ratio required by the standards – stirrups $\varnothing 8$ at 300 mm spacing)
N 1-4 G	–	N 3-4 G	
N 1-4 B	N 2-4 B	N 3-4 B	
N 1-1 G	N 2-1 G	N 3-1 G	Comparing to the reference value $\rho_w = 0.42\%$
N 1-1 B	N 2-1 B	N 3-1 B	

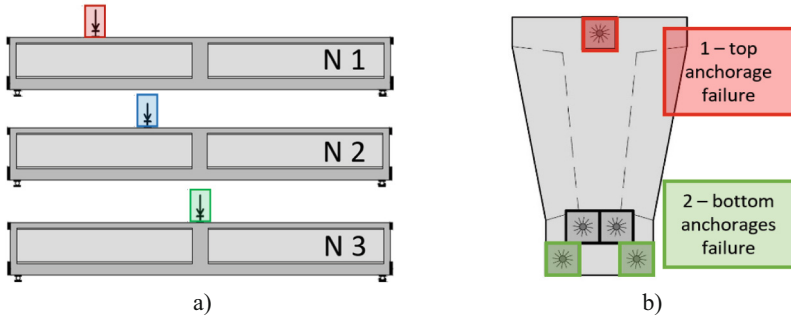


Fig. 2. (a) Analysed static schemes (vary a/d ratio); (b) exemplary anchorage failure indication.

3 Results of Numerical Analyses

Selected results of the numerical analyses are presented in this chapter. Figure 3 shows a comparison of the results of the numerical analyses with the corresponding experimental studies. The numerical calculation outcomes accurately reflect the experimental results. The difference between the experimental load capacity and corresponding numerical predictions did not exceed 5%.

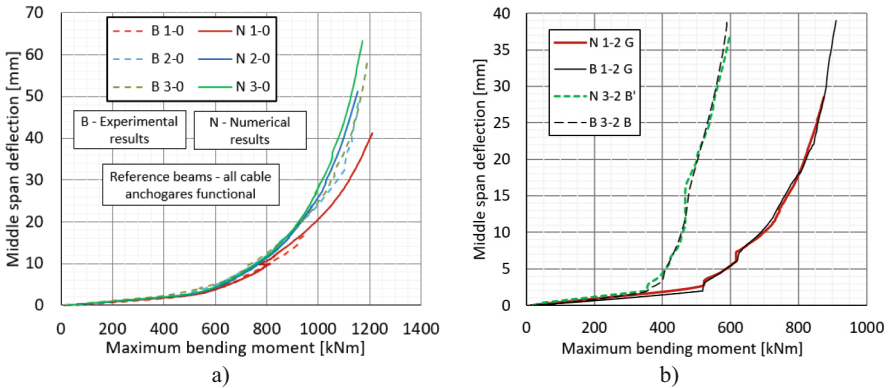


Fig. 3. Comparison of the experimental and the numerical results (deflection vs M_{\max}): (a) reference beams (all cable anchorages functional); (b) 2 bottom anchorages failure situation.

Figure 4 summarises the results of the major performed numerical analyses. A comparison of the reference models (with all functional prestressing cable anchorages) and the models with the two bottom anchorages failed is given – Fig. 4a presents a deflection increment at the midspan vs the maximum bending moment (at the external load application section), whereas Fig. 4b presents values of the deflection increment (at the external load application section) vs the maximum transverse force for models with reduced transverse reinforcement ratio.

All presented deflection values, indicate the increment relative to the beginning of the test. Thus, the zero deflection value refers to the prestressed element, with any damaged anchorages (if applicable), corresponding to the experimental results.

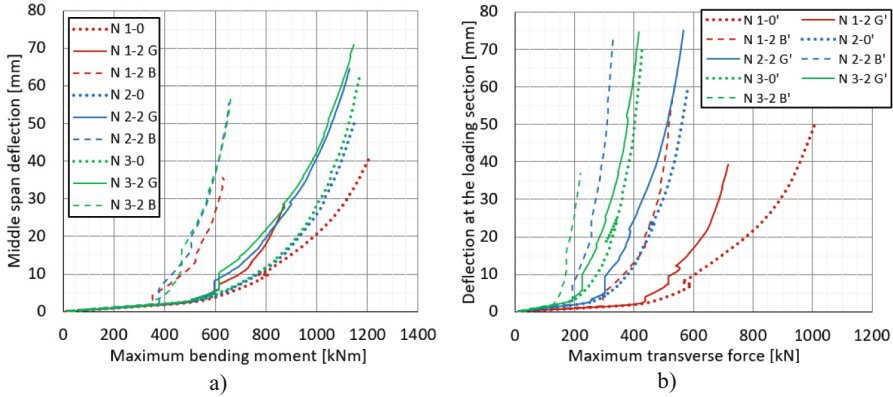


Fig. 4. Results summary of the numerical analysis: (a) middle span deflection vs M_{\max} (reference transverse reinforcement); (b) max deflection vs V_{\max} (reduced reinforcement ratio).

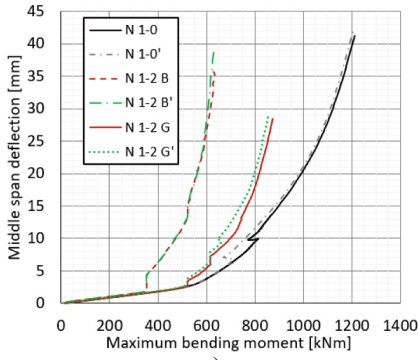
3.1 Transverse Reinforcement Ratio Effect Analysis

Figure 5 (at the next page) show a comparison of the calculation results for corresponding models with varying transverse reinforcement ratio (ρ_w). Numerical simulations of reference elements ($\rho_w = 0.42\%$) are compared with corresponding beam models with a transverse reinforcement ratio reduced by half. Plots of the deflection increment vs the maximum bending moment (in the external load application section) for shear slenderness a/d equal to 1.57; 2.61; 3.66 are shown in Fig. 5a; Fig. 5b and Fig. 5c, respectively.

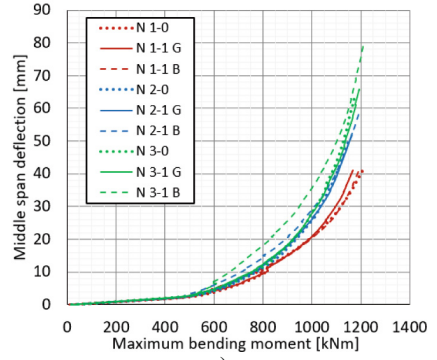
3.2 Effective Prestress Level Impact Analysis

The effective prestressing force magnitude analysis considered different scenarios of the prestressing cable anchorages failure (the number of damaged anchorages and their location), and the different quality of cable duct grout injection. Consequently, grouting quality determines the transmission length of prestressing force to the element after the anchorage failure and the effective prestressing force level.

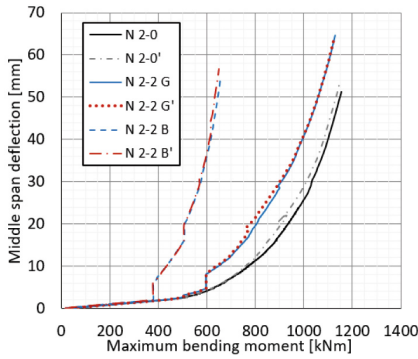
Figure 6 shows a comparison of the calculation results of reference numerical models (no damaged anchorages), with models with different combinations of damaged anchorages. The deflection increments at the middle span vs the maximum bending moment (in the external load application section) are shown. Figure 6a shows the results for models with top anchorage failure whereas Fig. 6b and Fig. 6c present the results for models with damaged bottom anchorages (the two lowest or all four bottom anchorages) for the cases of good (G - Fig. 6b) and bad (B - Fig. 6c) cable duct grouting quality, respectively.



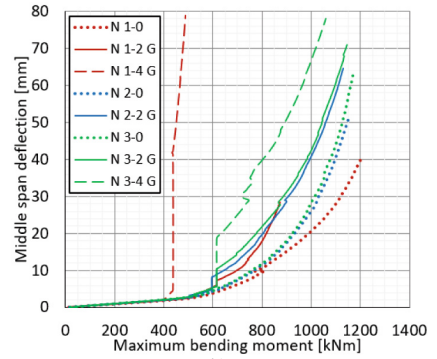
a)



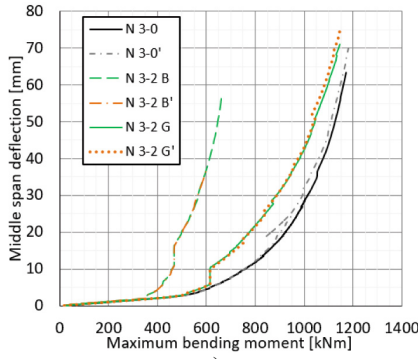
a)



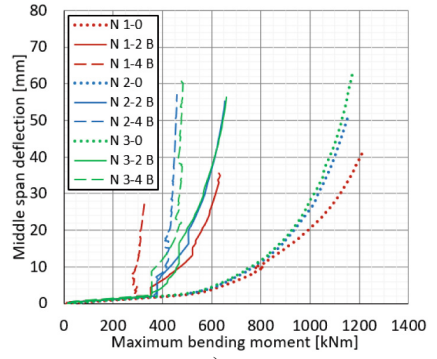
b)



b)



c)



c)

Fig. 5. Transverse reinforcement ratio effect analysis (deflection vs M_{max}) for a/d ratio value equal: (a) 1.57; (b) 2.61; (c) 3.66.

Fig. 6. Effective prestress level impact analysis, failure of: (a) top anchorage; or bottom anchorage for (b) G or (c) B grouting quality.

4 Discussion and Conclusions

The resulting differences in the capacity retrieved from the numerical model and the value obtained from the experimental tests are in the range of 0.3–4.1%. Whereas the differences for deflections at the failure load are in the range of 3.8–29.1%. The deviation of the mapping of deflections of elements is larger compared to the mapping of the failure load. However, it should be noted that the differences are at most several millimetres (maximum difference of 16 mm), which in global terms is an acceptable error. The results obtained demonstrate that nonlinear numerical modelling is a useful tool for the advanced evaluation process of existing building structures, especially in emergency situations. In addition, modelling is essential for cost-effective and efficient decision-making about the continued serviceability of structures.

The analyses of the transverse reinforcement ratio effect indicate that the stirrup reinforcement ratio does not significantly affect the ultimate load capacity. The load carrying capacity of modelled elements with reduced transverse reinforcement ratio compared to the reference elements differs by no more than 2% (excluding the capacity of N 3–2 B' model - a difference of about 9%). In any analysed case, no failure due to rupture of stirrups occurred. Moreover, the transverse reinforcement ratio does not show a significant effect on the increased strain or deflection increments.

Effective prestressing force analysis indicates that the load carrying capacity of elements modelled with a failure of anchorage for the top prestressing cable does not change significantly, regardless of the analysed quality of duct's grouting or the static scheme. The maximum differences in the load-carrying capacity of elements with a damaged top anchorage compared to the reference elements are $\pm 3.6\%$.

On the other hand, the load carrying capacities of modelled elements with damaged two bottom anchorages are reduced compared to reference models. The magnitude of the bearing capacity reduction is determined by the quality of cable duct grout injection. Elements with good grouting quality in cable ducts with damaged anchorages show a relatively small loss of capacity compared to the reference elements of 28% (for N 1–2 G) and 2% for higher shear slenderness (N 2–2 G and N 3–2 G). However, for members with bad cable duct grouting, the reduction in load capacity with reference models is very significant (nearly 50% for all shear slendernesses considered).

Models simulating the failure of four bottom anchorages of the prestressing cables indicate that until the crack initiation, the elements can carry loads. However, the further load bearing ability is significantly reduced.

Note that the case of the loss of the four anchorages of the bottom prestressing cables has not been tested experimentally. It should be acknowledged that the four bottom anchorages failure must be considered as an emergency condition.

5 Summary

The key findings of the numerical analyses are as follows:

- Transverse reinforcement ratio does not significantly affect the ultimate load capacity of the analysed elements. The ultimate load capacity of the elements with reference transverse reinforcement ratio compared to the elements with twice reduced stirrup ratio differs no more than 2%,

- Damage to the top anchors has a minor effect on the load-bearing capacity of the elements ($\pm 3.6\%$ margin),
- Ultimate load capacity of the elements with damaged bottom anchorages is significantly reduced (up to 28% - good grouting quality; 49% - bad grouting quality),
- The magnitude of the capacity loss is strongly determined by the quality of the cable duct grouting.

References

1. Muttoni A, Ruiz MF (2012) Levels-of-approximation approach in codes of practice. *Struct Eng Int* 22:190–194
2. Häussler-Combe U (2014) *Computational methods for reinforced concrete structures*, John Wiley & Sons, Ltd, ISBN 978-3-433-60361-1
3. Walraven J (2010) Residual shear bearing capacity of existing bridges. In: *Shear and punching shear in RC and FRC elements - fib bulletin No. 57*, pp. 129–138. International federation for structural concrete. ISBN 978-2-88394-097-0
4. Walczak R, Derkowski W (2022) Shear capacity tests of PC crane beams in uncertain prestressing tendons anchorage conditions. In: *Proceedings of the fib congress international federation for structural concrete*, pp 2045–2054
5. Derkowski W, Walczak R (2019) Problem of condition assessment of precast, posttensioned concrete crane beams in an extended period of use. In: *Proceedings of the fib symposium. International federation for structural concrete*, pp 1507–1514
6. Derkowski W, Walczak R (2020) Effect of shear span-to-depth ratio on posttensioned concrete crane beams shear capacity. *MATEC Web Conf.* 323:01019
7. Derkowski W, Sieriko R, Walczak R, Howiacki T, Bednarski Ł (2021) DFOS measurements for strain analysis of anchorage zone in 57-year-old posttensioned precast girder using static and high-frequency approach. *Struct Concr* 22(6):3414–3429
8. Walraven J, et al. (2013) *Fib model code for concrete structures 2010*. John Wiley & Sons, Ltd. International Federation for Structural Concrete. ISBN 978-3-433-60409-0
9. Maekawa K, Okamura H, Pimanmas A (2003) *Non-linear mechanics of reinforced concrete* CRC Press. ISBN 978-0-367-86555-9
10. Müller HS, Breiner R, Anders I (2013) *Fib bulletin No. 70 - code-type models for structural behaviour of concrete*. *Int Feder Struct Concr*. ISBN 978-2-88394-110-6
11. Maekawa K, Vecchio FJ, Foster S (2008) *Fib bulletin No. 45 - practitioner's guide to finite element modelling of reinforced concrete structures*. *Int Feder Struct Concr*. ISBN 978-2-88394-085-7
12. Vecchio FJ, Collins MP (1986) The modified compression field theory for reinforced concrete elements subjected to shear. *ACI J* 83(2):219–231
13. Vecchio FJ, Collins MP (1988) Predicting the response of reinforced concrete beams subjected to shear using modified compression field theory. *ACI Struct J* 85(3):258–268